Tiltrotor Whirl Flutter Analysis in Support of NGCTR Aeroelastic Wind Tunnel Model Design

Alessandro Cocco*, Pierangelo Masarati
Politecnico di Milano, Milano — Italy
* alessandro.cocco@polimi.it

Stefan van 't Hoff, Bart Timmerman
NLR — The Netherlands

Abstract

This work presents the modeling and preliminary whirl-flutter stability results achieved within the Advanced Testbed for TILtrotor Aeroelastics (ATTILA) CleanSky2 project. ATTILA entails the design, manufacturing and testing of a semi-span wind tunnel model of the Next Generation Civil TiltRotor. A description of the preliminary MBDyn and FLIGHTLAB multibody models is presented. The modelling technique of each subcomponent of the model, namely the wing, the rotor, the blades and the yoke is briefly illustrated. The predicted dynamic characteristics of the wing-pylon system and the rotor are then compared. Finally, some preliminary whirl-flutter stability predictions are presented, along with the techniques that will also be used in the wind tunnel tests to identify the aeroelastic modes of the model.

1 INTRODUCTION

Owing to their outstanding capability of taking off and landing vertically and, at the same time, achieving high speeds in forward flight, tiltrotor aircraft received increasing attention over the past decades.

After a development phase that encompassed two experimental aircraft that successfully made it to flight (the Bell XV-3 and XV-15) and other less fortunate technology demonstrators, the concept finally proved its soundness with the Bell-Boeing V-22, a military aircraft that has been operated with increasing reward for the last 20 years. With the then Bell-Agusta and now Leonardo AW609 poised to become operational, the tiltrotor design is mature enough to enter the civil air transport market [1].

Nevertheless, tiltrotor design is still a challenging engineering task, considering the multipurpose missions that are expected to be accomplished by this complex type of aircraft. In particular, the problem of assessing whirl flutter stability limits is at the same time fundamental and challenging. Whirl-flutter is an aeroelastic stability phenomenon that is known to affect both turboprop and tiltrotor aircraft [2]. When a rotor mounted on a flexible structure rotates, the normal vibration modes associated with the elastic behaviour of the supporting structure may interact with the precession motion of the rotor.

When its motion is perturbed, each point on the rotor axis of rotation draws paths about its reference position. This motion changes the way each rotor blade is affected by the incoming airspeed, correspondingly altering the overall aerodynamic loads. At the verge of whirl flutter, when this phenomenon is triggered, perturbations result in a periodic orbit. The resulting forces can lead to the divergence of the system response, in what is a truly aeroelastic instability [3].

Nowadays, although the phenomenon in tiltrotor aircraft is understood, the capability to predict it is still limited, despite the availability of sophisticated aeroelastic analysis tools. The difficulty lies in its dependence on many factors. For instance, the geometrical design, structural properties, actuator dynamics, etc. can all contribute to the whirl flutter characteristics in manners that are not always intuitive.

As a consequence, the possibility to validate numerical predictions using experimental data is of paramount importance from an industry standpoint.

This work is intended to present the preliminary modelling efforts made for the Next-Generation Civil Tilt Rotor-Technology Demonstrator (NGCTR-TD) wind tunnel testbed, within the CleanSky2 project ATTILA. Numerical models of the reference testbed have been developed using MBDyn[1] [4] and FLIGHTLAB[2], respectively by collaborating research teams at Politecnico di Milano (POLIMI)and the Royal Netherlands Aerospace Centre (NLR).

The models are being exploited to support the design of the physical wind tunnel testbed. Pending experimental characterization of the ATTILA testbed dynamics, code-to-code verification results are presented and compared with data obtained from a reference CAMRAD II model of the full-scale aircraft. Finally, preliminary whirl flutter predictions are presented.

[1] http://www.mbdyn.org/, last accessed February 2021.
[2] http://www.flightlab.com/

Presented at the 47th European Rotorcraft Forum, Glasgow, UK, 7–10 September, 2021
This work is licensed under the Creative Commons Attribution International License (CC BY). Copyright © 2021 by authors.

2 MULTIBODY TOOLS

2.1 MBDyn

MBDyn automatically writes and solves the equations of motion of a system entities possessing degrees of freedom - nodes - connected through algebraic constraints, and subjected to internal and external loads. Constraint equations are explicitly taken into account, following a redundant coordinate set approach. Thus, the resulting system of Differential-Algebraic Equations (DAEs) is in the form

$$\mathbf{M}(\mathbf{x},\mathbf{t})\dot{\mathbf{x}} = \mathbf{p} \tag{1a}$$

$$\dot{\mathbf{p}} = \phi^{T}_{/\mathbf{x}}\lambda + \mathbf{f}_i(\dot{\mathbf{x}},\mathbf{x},t) + \mathbf{f}_e(\dot{\mathbf{x}},\mathbf{x},t) \tag{1b}$$

$$\phi(\mathbf{x}) = \mathbf{0} \tag{1c}$$

where $\mathbf{x}$ are the kinematic unknowns, $\mathbf{p}$ the momentum unknowns, λ the algebraic Lagrangian multipliers, $\mathbf{M}$ is a configuration and time dependent inertia matrix, $\mathbf{f}_i, \mathbf{f}_e$ are arbitrary internal and external forces, $\phi(\mathbf{x})$ are the nonlinear algebraic constraint equations (holonomic constraints) and $\phi^{T}_{/\mathbf{x}}$ is the Jacobian matrix of the holonomic constraints with respect to the kinematic unknowns. Each node instantiates the writing of balance equations (1b), while only nodes to which inertia properties are associated instantiate the writing of momenta definitions (1a). Additional states, associated with scalar fields (namely, hydraulic pressure, temperature, electric current) and thus the associated differential balance equations, can be taken into account through a specialized set of nodes.
Elements are responsible for the contributions to the balance equations through (visco)elastic internal forces $\mathbf{f}_i$, possibly state-dependent external force fields $\mathbf{f}_e$ (e.g. aerodynamic forces) and reaction forces, introduced by means of the Lagrange multipliers λ and the gradient of the nonlinear algebraic constraint equations 1c.
The DAE system can be integrated with several different A/L stable integration methods, among which an original multistep method with tunable algorithmic dissipation, specifically designed for the class of problems MBDyn is usually asked to tackle.

2.2 FLIGHTLAB

FLIGHTLAB is a state-of-the-art multi-body, component-based, selective fidelity modeling and analysis software package. It supports modeling and simulation of rotorcraft, fixed-wing aircraft, compound aircraft, helicopters, multicopters, drones, flying cars and experimental aircraft configurations.

Rotorcraft and other aircraft models can be developed to fit their application with the desired level of fidelity. Depending on the fidelity, the numerical models can be used for engineering analysis, real time simulation, or both. The development system is also used to generate run-time models for real time applications.

The key capabilities of the software include:

- Multiple bodies, multi-body dynamics
- Nonlinear unsteady aerodynamics
- Flight dynamics and real time simulation (including full flight simulators)
- Flight performance, stability, controllability, and handling qualities
- Aeroelastic stability, vibration, and loads
- Aircraft systems analysis and hardware-in-the-loop (HIL) simulation
- Couple with external programs including CFD and Matlab/Simulink

3 MODEL DESCRIPTION

The entire model can be divided into two major subcomponents: the wing-pylon assembly and the rotor. A render of the ATTILA multibody model is showed in fig. 1.

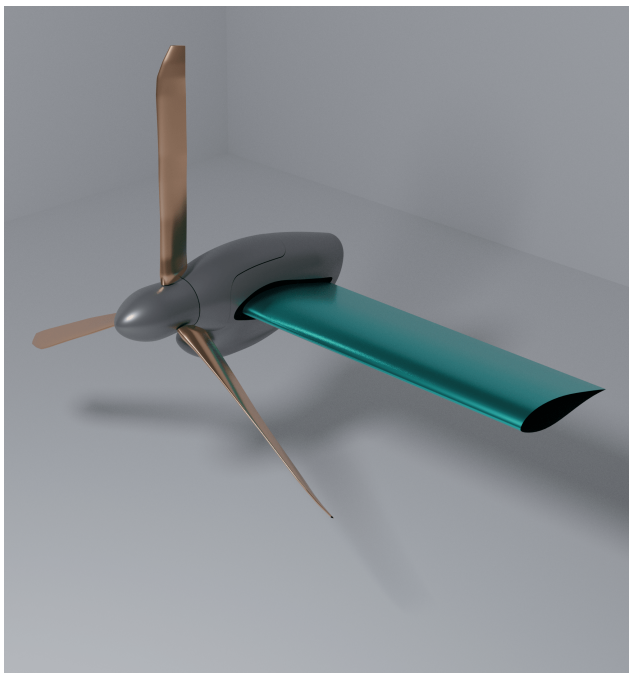

Figure 1: Render of the ATTILA multibody model

3.1 WING-PYLON MODEL

The wing-pylon model has been developed with the aim to reproduce the fundamental frequencies and mode shapes of an equivalent finite element stick model that has been tuned to match the full-scale aircraft dynamics at the rotor hub.

In MBDyn, the wing model is composed with 3 finite volume three-node beam elements [5] for the stiffness part, and one body element for each node to model the inertial component. The nacelle part is divided into a tilting and non-tilting part, both of which are considered as rigid body.

The parts are connected by means of deformable joints representing the flexibility of the down-stop and the wing-pylon attachment. The aerodynamics are introduced through the MBDyn aerodynamic beam. Each aerodynamic beam has been linked to the corresponding structural beam.

The FLIGHTLAB model contains 16 elastic beam segments for the wing and 4 beam segments for the nacelle. The wing airloads are modelled using an enhanced lifting line model with a Peters He [6] finite-state wake.

Each structural beam segment is connected to a quasi-steady airloads component, which uses 2D (AoA, Mach/Reynolds) table look-up to calculate the airloads.

The connection between the wing and the nacelle is modelled by three torsional spring-damper components that are collocated and connected in series.

The nacelle tilting hinge is modelled by a gimbal hinge, with a pitch-yaw stiffness that can be changed at run-time to switch between the downstop ON and OFF configurations.

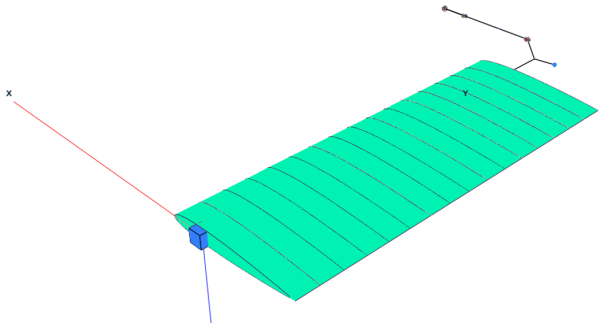

Figure 2: FLIGHTLAB Wing-Pylon model

3.2 ROTOR MODEL

The ATTILA proprotor is a three bladed stiff-in-plane rotor with a gimballed hub. It is formed by the control chain, three blades and the yoke.

3.2.1 MBDYN

The blade and the yoke are modelled in MBDyn using the three-node beam element, similar to the modelling of the wing.

In order to capture the orthotropic behavior of the blade and the yoke, the stiffness matrix has been constructed in such a manner that it incorporate the offsets and relative rotations between the feathering axis and the neutral and elastic axis.

The aerodynamic model is constructed using the MBDyn aerodynamic beam. Each aerodynamic panel can incorporate aerodynamic twist variation and profile transitions. Along the blade, six airfoils are placed with non-smooth transition.

The blade is connected to the yoke in two locations, at the inner bearing and at the outer bearing. In MBDyn, these two bearings are modelled with ideal rigid constraints: for the inner bearing both flapwise and chordwise displacement are constrained, for the outer bearing all three translations are constrained.

The control chain has a traditional helicopter-like configuration: it is formed by seven MBDyn nodes joined following the scheme of Fig. 4.

- `Pylon`: this node represents the physical connection between the pylon extremity and the rotor; when the isolated rotor is analysed this node is clamped.

- `Airframe`: this node is the one to which the commands (cyclics and collective) are imposed, in order to decouple the two cyclic inputs the node is positioned on a reference system that is rotated by the angle $\psi_{sp} = atan\left(\frac{x_{sp}}{y_{sp}}\right)$ where x_{sp} and y_{sp} are the locations of the pitch link attachment to the swashplate.

- `Fixed Swashplate`: this node is rigidly constrained in the in-plane translations and the axial rotation to the airframe. To account for the flexibility of the control chain, a collective spring and two cyclic springs are positioned in between the airframe node and the fixed swashplate.

- `Rotating Swashplate`: this node is connected to the fixed swashplate by means of a revolute hinge; it is positioned on a rotating reference system.

- `Engine`: this node is connected to the mast by means of a torsional spring in order to reproduce the drive-train dynamics.

- `Mast`: this node transmits the rotation to the hub and to the rotating swashplate. It is connected to the pylon node by means of a revolute hinge.

- `Hub`: This node is constrained to the mast node by means of a spherical hinge and a MBDyn gimbal rotation: the combination of these two joints creates an ideal constant velocity joint.

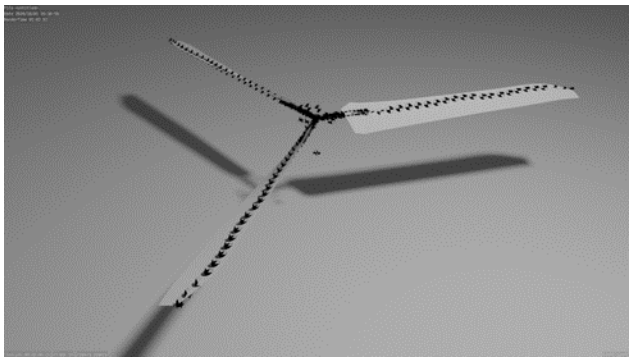

Figure 3: MBDyn rotor model

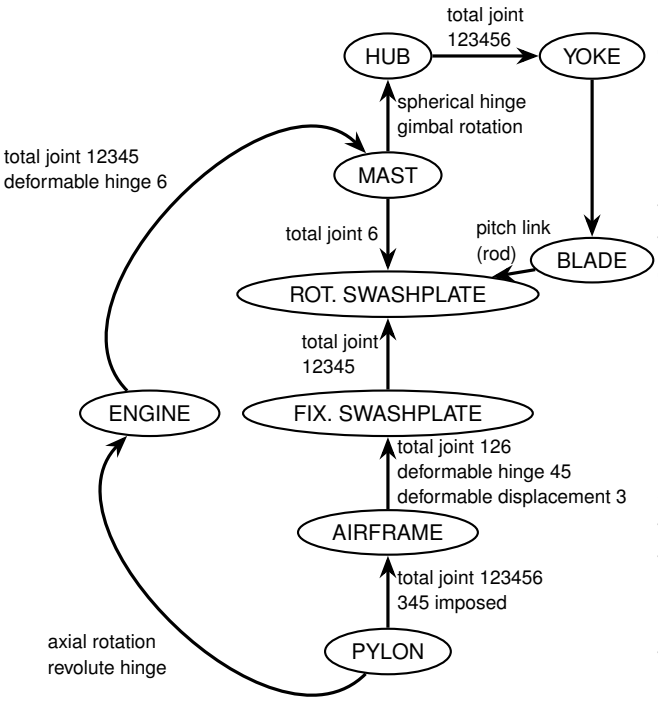

Figure 4: Flowchart indicating the individual blade pitch control system components and their connections

3.2.2 FLIGHTLAB

In FLIGHTLAB, the blade is modelled using elastic beam components. The beam axis of each finite element is defined by the locus of shear centers (the elastic axis) of the physical blade. Appropriate sweep and droop rotations are applied to approximate the position of the elastic axis with respect to the feathering axis.

The aerodynamics of the blade are modelled by means of table look-up with a correction for unsteady circulatory effects. The transition between the airfoils is non-smooth. Provisionally, the induced velocity is modelled as a uniform inflow with Glauert distribution.

The blade is connected to the yoke at two locations, at the inner bearing and at the outer bearing. This creates a dual load path. The FLIGHTLAB solver is single load path based, where calculations are performed sequentially from the tip of the blade towards the rotor hub. To facilitate the dual load path introduced by the combination of the blade and the yoke, the root-end of the blade is modelled as a separate beam that is inverted and connected at the physical root via 2- parent springs representing the inner bearing. In this set-up, the root of the torque tube acts as a second "blade tip" as far as the solver is considered.

The main "blade" load path consists of the yoke segments and the blade segments outboard from the outer bearing. The torque tube load path consists of the blade segments between the inner and outer bearings. The outer bearing is modelled as a series of three hinges with zero spring stiffness, allowing rotation around all three axes, but constraining translation. Due to the single load path nature of the FLIGHTLAB solver, the inner bearing cannot be modelled as a hinge-slide combination. Instead, two perpendicular rigid flap/lag offsets are placed at the location of the inner bearing, perpendicular to the yoke. The inboard end of the torque tube is then connected to the rigid offsets through two 2-parent translational linear spring-dampers that only constrain translation. The springs have been assigned high stiffness to approximate a rigid constraint. Both the springs and the rigid offsets are identical in length. The length of the spring is arbitrary, but large enough to minimize the spring restraint in the axial direction of the yoke in the presence of relative displacements/rotations.

As mentioned, there are two offset/spring combinations: one in the flapwise direction and one in the edgewise direction. In this way, translation of the inboard end of the torque tube is constrained to the yoke at the position of the inner bearing, both in flapwise and edgewise direction. Due to the length of the springs and rigid offsets, the angle between them will be small, resulting in very small off-axis forces. As such, translation in the spanwise direction is nearly unobstructed, whereas rotation is free in all axes.

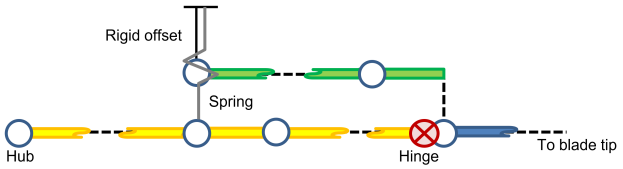

Figure 5: FLIGHTLAB dual load path modelling. Nodes (white), hinge (red), yoke segments (yellow), blade segments (blue) and torque tube segments (green).

In FLIGHTLAB the control chain is modelled as a conventional swashplate arrangement. The rotor hub is rigidly connected to the tip of the pylon shaft when analyzing the half-wing model, and rigidly connected to the inertial system when analyzing the isolated rotor. A bearing component drives the rotor rotation over the gimbal, which is connected to the yoke via an underslung offset.

The swashplate is located above the hub, connected via a rigid offset. The non-rotating swashplate node is connected to the pylon through a translational linear spring-damper, representing the collective spring stiffness of the control chain. A collocated gimbal hinge with spring-damper effects models the cyclic pitch spring stiffness.

The non-rotating swashplate node translates along the shaft axis in accordance with the collective input through a controlled slider. Azimuthal rotation of the rotating swashplate node is achieved by a controlled hinge, which is slaved to the rotational speed of the hub. The swashplate mass is fixed to the rotating swashplate node and is required to avoid a singular matrix during linearization. Each pitch link is connected to the rotating swashplate and offset from the shaft through azimuthal rotation and rigid translation. Cyclic

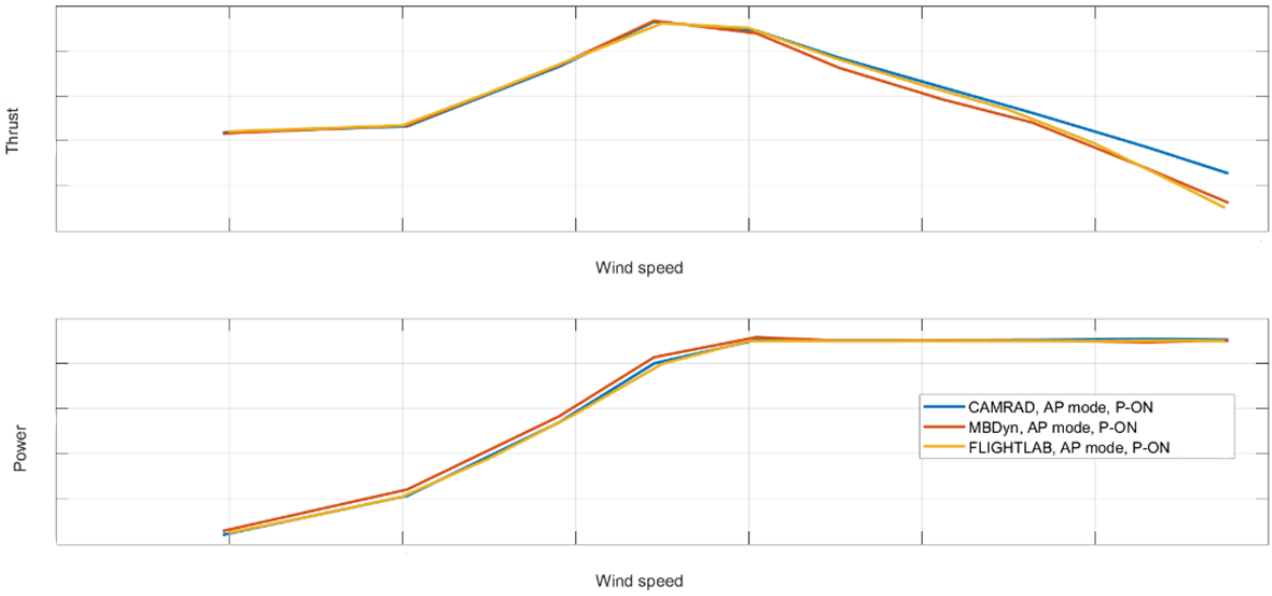

Figure 7: Trim comparison between CAMRADII, FLIGHTLAB and MBDyn

control inputs are introduced at the root end of the pitch links through a controlled slider. A 2-parent linear spring-damper represents the pitch link stiffness and is connected to the pitch horn on the blade. The pitch link spring does not constrain rotation.

4 MODEL VALIDATION

4.1 WING-PYLON

In order to validate the wing-pylon model, a modal analysis has been performed comparing the frequencies and mode shapes of both the MBDyn and FLIGHTLAB models with a target NASTRAN stick model.

At this stage, the comparison of the mode shapes is based on the Modal Assurance Criterion (MAC) defined by Eq. (2). In this equation ψ_i^{FEM} represents the $i-th$ mode shape calculated using the original finite element stick model, whereas the term ψ_j^{MBD} represents the $j-th$ mode shape obtained from the two multibody codes.

$$(2) \quad MAC(i,j) = \frac{|(\psi^{FEM})_i^T (\psi^{MBD})_j|^2}{[(\psi_i^{FEM})^T (\psi_i^{FEM})][(\psi_j^{MBD})^T (\psi_j^{MBD})]}$$

The MAC matrix results are presented in Fig. 6. The differences between the MBDyn/FLIGHTLAB models and NASTRAN are negligible. Close inspection of the 6-DOF mode shape at the location of the rotor hub confirms the satisfactory correlation.

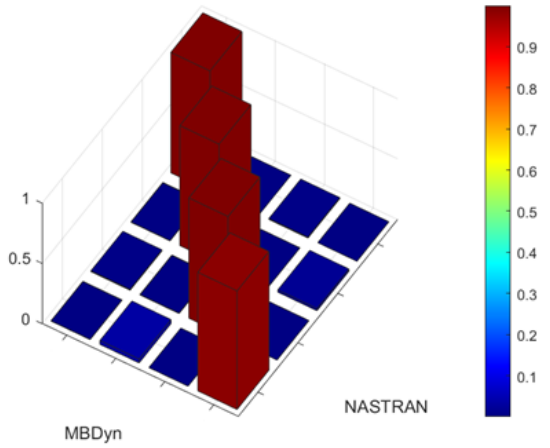

Figure 6: Wing-pylon downstop ON MAC comparison of MBDyn and NASTRAN

4.2 ROTOR

To validate the dynamic behavior of the rotor in vacuum, the rotor frequencies at different collective pitch have been evaluated and compared to the fan plots obtained with the equivalent full-scale CAMRADII rotor model.

Moreover, the rotating blade mode shapes have been compared for different collective angles and with and without the presence of the drive train system. Remarkably good agreement has been obtained between the three models, despite their relative complexity.

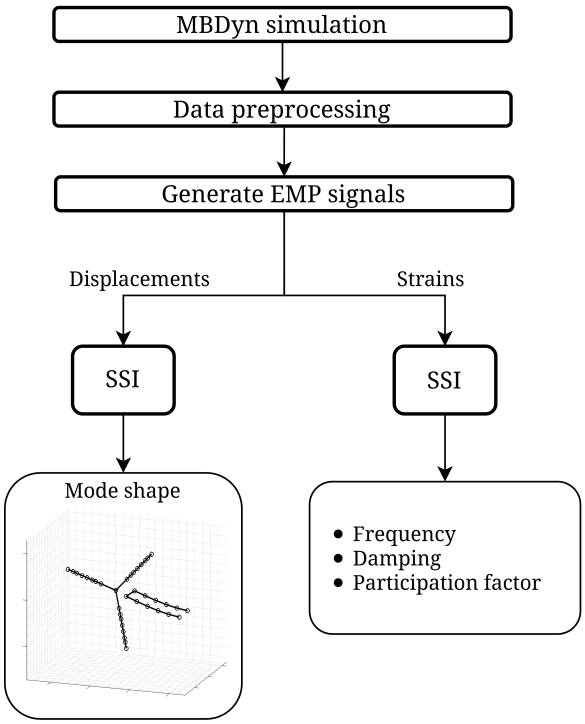

(a) POMA method analysis procedure

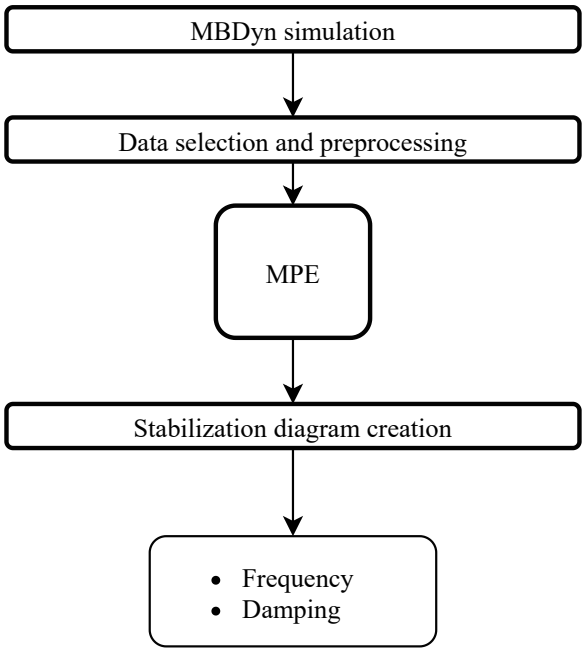

(b) MPE method identification process flowchart

Figure 8: Identification methods flow charts

4.3 TRIM PROCEDURE

The trim targets depend on the configuration being investigated, but are identical for both FLIGHTLAB and MBDyn. Power-on trim is based on achieving a target thrust and zero cyclic gimbal flap until the maximum torque is reached. At that point, a constant torque trim is maintained to represent a steady powered descent. During power-off trim the rotor is de-clutched from the engine (i.e., no torque is transmitted) and the rotor speed is held constant.

Figure 7 presents a comparison of the trim results for the power-on configuration. In FLIGHTLAB, trim is achieved by a gradient-based iteration process. In power-off trim, the rotor speed is frozen at the target value and the swashplate controls are adjusted to achieve an average rotor azimuthal acceleration equal to zero. Post-trim, the rotor speed is released, and the collective is fine-tuned to achieve the desired steady power-off rotor speed.

In MBDyn, power-on trim is achieved by starting from an initial guess of the collective angle and then applying the desired torque at the engine side. The desired rotor speed is maintained using a PI controller that sets the appropriate swashplate collective displacement. The power-off condition is achieved simply by setting the applied torque to zero.

5 WHIRL FLUTTER PREDICTION

5.1 FLIGHTLAB

The whirl flutter analysis in FLIGHTLAB is performed through direct linearization from trim by means of central difference perturbation of the 1^{st} and 2^{nd} order states. This technique permits to identify the wing-pylon, drive system and rotor modes, providing valuable information about the underlying dynamics.

A nonlinear excitation-based analysis replicating the expected wind tunnel test procedure has also been implemented to verify the linearization results, investigate various experimental excitation strategies, and determine the required excitation magnitude and the associated structural loads.

5.2 MBDYN

In MBDyn the stability analysis of the whole tiltrotor model is analyzed following two approaches:

- Matrix Pencil Estimation (MPE), performed in order to retrieve the main wing modes.
- Periodic Operational Modal analysis (POMA), performed in order to take into account the periodicity of the system with the purpose to extract not only the wing main harmonics but also the corresponding superharmonics.

5.2.1 Matrix Pencil Estimation

The Matrix Pencil Estimation method (MPE) was designed by Hua et al. [7] to estimate parameters of exponentially damped or undamped sinusoids in the presence of noise. A multiple input algorithm was further proposed by Favale et al. [8] who applied the methodology also in more complex problems, such as tiltrotor whirl flutter analysis. The method can estimate the modal parameters of a system from its free responses to an external input.

Starting from a multibody simulation of the full semi-span tiltrotor wind tunnel model, excited using sinusoidal input at the swashplate, all the available values of strain in the beam elements and accelerations of the nodes are extracted. A selection process is then performed to ensure a reliable identification and select the most meaningful data. After a simple data pre-processing, consisting of filtering and re-sampling, the identification algorithm is applied to compute the poles of the system. A further post-processing step, involving the creation of stabilization diagrams, as suggested in [8], is finally executed to evaluate the quality of the identification process and retrieve the desired results, such as frequency and damping ratio.

5.2.2 Periodic Operational Modal Analysis (POMA)

Rotorcraft modal identification is typically performed in non-rotating coordinates by applying a multiblade coordinate transformation (MBC). However, when dealing with real-world problems a number practical issues may arise due to, e.g., small anisotropy of the rotor blades, or slightly different axial position of the sensors on each blade. In addition, when performing a periodic stability analysis, a richer insight in system behaviour can be retrieved: for each harmonic captured with a MBC transformation approach a set composed by a, theoretically, infinite number of harmonics is obtained.

For the present work the algorithm called Periodic Operational Modal Analysis (POMA) originally proposed by Werely and Hall [9] was used. It is based on the harmonic transfer function concept that is the periodic counterpart of the frequency response function for LTI systems. Werely defined a new fundamental signal space for periodic systems containing the so-called exponentially modulated periodic signals (EMP). These have been defined as the complex Fourier series of a periodic signal of frequency ω_p, modulated by a complex exponential signal:

$$u(t) = \sum_{n \in Z} u_n e^{s_n t} \tag{3}$$

where $s_n = s + n j \omega_p$ and u_n are Fourier coefficients of $u(t)$. Then we can define the harmonic transfer function as:

$$y(\omega) = G(\omega) u(\omega) \tag{4}$$

In theory $G(\omega)$ should be an infinite matrix in order to consider all the harmonics that characterize an LTP system. However, for most applications a satisfactory approximation can be obtained with a limited or even small number of harmonics.

The main assumption on which the applied method is based is that the input spectrum should be relatively flat in the range of frequencies of the modes of interest. Under this hypothesis, the ATTILA wing-pylon model in MBDyn was excited by superimposing a white noise disturbance to the components of the wind speed. The strains and displacements were then pre-processed to remove any offsets in order to retrieve zero-mean signals. The signals were then exponentially modulated. Finally, a Stochastic Subspace Identification (SSI) [10, 11] algorithm was applied to identify the frequency and damping from the strain output, and the mode shapes from the displacements.

In synthesis, the proposed identification technique can be summarized by the following steps:

- Record the response $y(t)$ of the system to a broadband input
- Exponentially modulate the response $y(t)$ to generate the signals $\hat{y}_n(t) = y(t) e^{-in\omega_p t}$. The value of n ranges from $-\frac{n_h - 1}{2}$ to $\frac{n_h - 1}{2}$, where n_h is the maximum number of Fourier coefficients, equal to the number of harmonics, used to approximate system's periodicity.
- Compute the autospectrum of $\hat{y}(t)$ using a standard approach (e.g. Welch's method).
- Apply classical identification techniques to extract the system modal parameters. In this work, a covariance-driven stochastic subspace identification (cov-SSI) algorithm has been applied.

6 RESULTS

Figure 9 shows the whirl flutter stability predictions for the power-on configuration in airplane mode with the downstop engaged. The figure compares the FLIGHTLAB modes identified through a direct linearization and the MBDyn modes identified through the Periodic Operational Modal Analysis.

The two codes shows a similar trend for the wing bending mode (red) and the wing chord mode (blue). The FLIGHTLAB model predicts a lower damping value when considering the torsional mode (black) and pylon-yaw mode (cyan).

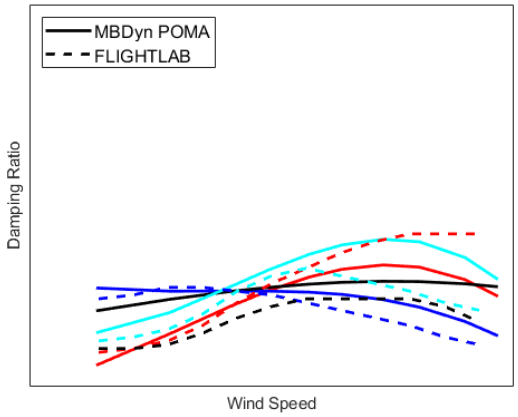

Figure 9: Power-ON configuration: comparison between FLIGHTLAB and MBDyn identified through POMA. Wing bending (red), wing chord (blue), wing torsion (black) and pylon-yaw (cyan)

Figure 10 shows the comparison between the two identification algorithms adopted for the MBDyn model. The firsts three modes (wing bending, wing chord and wing torsion) show a good match. A non-negligible difference is found for the pylon yaw mode. The damping curve predicted by the MPE method changes slope at a lower speed when compared to the POMA method. This discrepancy may be due to the different excitations used for the two methods. That is, since the system is nonlinear, the modal response may be different when excited by turbulence rather than a deterministic excitation applied to the swashplate.

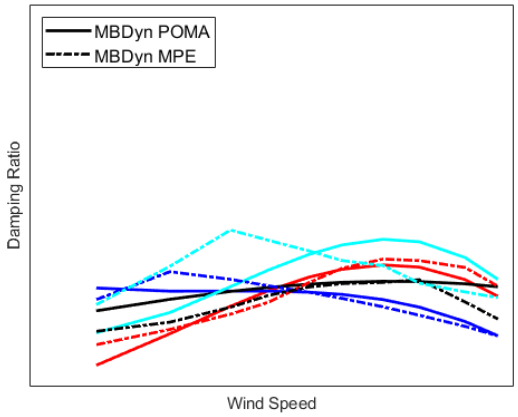

Figure 10: Power-ON configuration: comparison between MBDyn POMA and MPE comparison. Wing bending (red), wing chord (blue), wing torsion (black) and pylon-yaw (cyan)

Figure 11 shows the whirl flutter stability predictions for the power-off configuration in airplane mode. The comparison between MBDyn (identified through the POMA method) and FLIGHTLAB exhibits an overall good agreement. In this case the wing bending mode identified in FLIGHTLAB shows a slightly stepper slope with respect to MBDyn, whereas the damping predicted for the pylon yaw mode is higher in the MBDyn model. The wing chord and torsion modes, instead are almost perfectly matched.

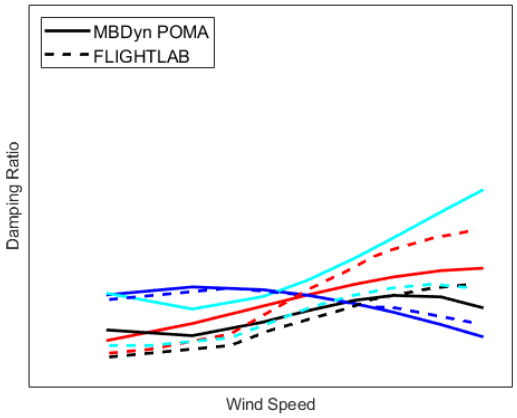

Figure 11: Power-OFF configuration: comparison between FLIGHTLAB and MBDyn identified through POMA. Wing bending (red), wing chord (blue), wing torsion (black) and pylon-yaw (cyan)

Figure 12 shows the comparison of between the two identification algorithms adopted in MBDyn. In this case the wing beam bending and the wing chord modes are almost in a perfect agreement. The wing torsion mode does not show a change in slope when it is identified through the MPE method. As in the power-on configuration, the pylon-yaw mode shows a different trend between the two identification methods.

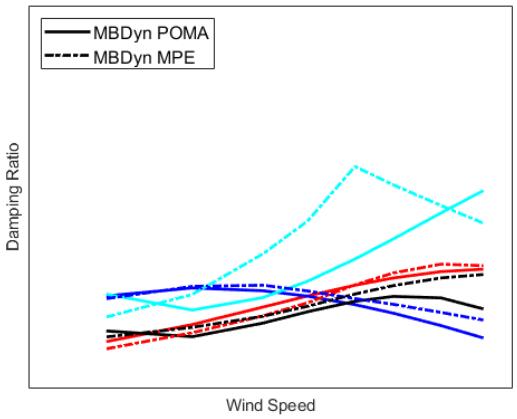

Figure 12: Power-OFF configuration: comparison between MBDyn POMA and MPE. Wing bending (red), wing chord (blue), wing torsion (black) and pylon-yaw (cyan)

7 CONCLUSIONS

Two multibody models of the Next-Generation Civil TiltRotor-Technology Demonstrator (NGCTR-TD) wind tunnel testbed have been independently developed using FLIGHTLAB and MBDyn. Both models are in good agreement with the reference rotor CAMRAD II model and NASTRAN wing-pylon stick model.

The experimental set-up has been assessed by utilizing three methods for the identification of the flutter modes. The first is based on state linearization as adopted in FLIGHTLAB. In MBDyn, the Matrix Pencil Method and Periodic Operational Modal Analysis have been applied.

The comparison between FLIGHTLAB and MBDyn shows good agreement for the wing beam bending, chord and torsion modes, with more evident discrepancies for pylon-yaw. The discrepancies are attributed to differences in the underlying modelled dynamics and not the identification methodologies.

The POMA method has the advantage of be able to extract the mode shapes of both the wing-pylon and rotor mode shapes relatively easily. Their visualization grants the possibility to deeper understand the system behaviour and instability mechanisms.

Acknowledgments

The research leading to these results has received funding from the Clean Sky 2 – H2020 Framework Programme, under the grant agreement N.863418, (the ATTILA project).

Copyright Statement

The authors confirm that they, and/or their company or organization, hold copyright on all of the original material included in this paper. The authors also confirm that they have obtained permission, from the copyright holder of any third party material included in this paper, to publish it as part of their paper. The authors confirm that they give permission, or have obtained permission from the copyright holder of this paper, for the publication and distribution of this paper as part of the ERF proceedings or as individual offprints from the proceedings and for inclusion in a freely accessible web-based repository.

REFERENCES

[1] ACARE — Report of the Group of Personalities. European aeronautics: a vision for 2020, January 2001.

[2] Jiří Čečrdle. Whirl flutter-related certification according to FAR/CS 23 and 25 regulation standards. In *IFASD 2019*, Savannah, Georgia, USA, June 9–13 2019.

[3] Wilmer H Reed. *Review of propeller-rotor whirl flutter*. National Aeronautics and Space Administration, 1967.

[4] Pierangelo Masarati, Marco Morandini, and Paolo Mantegazza. An efficient formulation for general-purpose multibody/multiphysics analysis. *J. of Computational and Nonlinear Dynamics*, 9(4):041001, 2014. doi:10.1115/1.4025628.

[5] Gian Luca Ghiringhelli, Pierangelo Masarati, and Paolo Mantegazza. A multi-body implementation of finite volume beams. *AIAA Journal*, 38(1):131–138, January 2000. doi:10.2514/2.933.

[6] David A Peters, David Doug Boyd, and Cheng Jian He. Finite-state induced-flow model for rotors in hover and forward flight. *Journal of the American Helicopter Society*, 34(4):5–17, 1989.

[7] Yingbo Hua and Tapan K Sarkar. Matrix pencil method for estimating parameters of exponentially damped/undamped sinusoids in noise. *IEEE Transactions on Acoustics, Speech, and Signal Processing*, 38(5):814–824, 1990.

[8] P. Pivetta, A. Trezzini, M. Favale, C. Lilliu, and A. Colombo. Matrix pencil method integration into stabilization diagram for poles identification in rotorcraft and powered-lift applications.

[9] Norman M. Wereley. *Analysis and control of linear periodically time varying systems*. PhD thesis, Massachussets Institute of Technology, 1991.

[10] C. Rainieri and G. Fabbrocino. Influence of model order and number of block rows on accuracy and precision of modal parameter estimates in stochastic subspace identification. *Influence of model order and number of block rows on accuracy and precision of modal parameter estimates in stochastic subspace identification*, 2014.

[11] S. Chauhan. Subspace algorithms in modal parameter estimation for operational modal analysis: Perspectives and practices.